Applied Mathematics & Information Sciences
An International Journal

http://dx.doi.org/10.18576/amis/200507

Analytical Solutions for Nuclear Magnetic Resonance Signal Bloch Equations with Varied Magnetic Excitation and Frequency Phase Shift

Nadia Boutabba[1], *Sofiane Grira*[2] *and Hichem Eleuch*[1,*]

[1] Univ. Polytechnique Hauts-de-France, LAMIH, CNRS, UMR 8201, F-59313 Valenciennes, France
[2] Al Akhawayn University, Ifrane, Morocco

Received: 7 Jun. 2026, Revised: 20 Jul. 2026, Accepted: 28 Aug. 2026
Published online: 1 Sep. 2026

Abstract: Modern Nuclear Magnetic Resonance NMR research is highly interested in Bloch equation solutions and their dynamical evolution using pulse sequences under static or variable radio-frequency ”RF” fields. Sophisticated combinations of these pulses enable the manipulation and extraction of information about the behavior of spin systems. Nonetheless, few analytical exact solutions to Bloch equations exist to the best of our knowledge. In this context, our research investigates exact analytical solutions of Bloch equations governing nuclear magnetic resonance NMR signals in response to an external magnetic field. We address the case where external radio-frequency magnetic field strength is time-dependent, the magnetization of the medium (which is experimentally equivalent to a spectrometer magnetic field) is also a time-variable, and, the frequency shift caused by spatial variations in the magnetic field is chirped. Hence, the temporal dynamics of spin magnetization components are fully determined. These solutions are in terms of the RF magnetic field, the relaxation times T_1 and T_2 (representing the rates at which the longitudinal and transverse magnetization recover or decay, respectively), and the frequency shift. Finally, we numerically derive these signals for two RF excitations: Eburp and Sine, which we compare to our exact solutions (denoted by the EX pulse). Interestingly, we observe that the magnetization signal is almost identical for Eburp and EX pulses while the absorption and dispersion are similar for a short excitation time.

Keywords: Bloch Equations, Nuclear Magnetic Resonance, Exact Analytical Solutions

1 Introduction

In the physics of nuclear magnetic resonance *NMR*, Felix Bloch, in 1946 [3] derived a set of equations to describe the time dependence of the net magnetization in terms of the magnetic field and the relaxation time. This relaxation time refers to the energy released to the environment by the spin. Bloch introduced two relaxation time constants, denoted by T_1 and T_2 representing the rates at which the longitudinal and transverse magnetization recover or decay, respectively. Besides, these relaxation time constants are critical in understanding various NMR processes of biological cells and tissues. Indeed, by extracting the information from the Bloch equations describing the NMR signal under a weak radio frequency magnetic field $''RF''$, we can understand the relative clinical state of the biological cells[2].

The first solution to the Bloch equations describing the magnetization components of a spin ensemble, was proposed by Torrey in the late 1949[27]. The spin-spin time constant T_2 (the time needed for a nuclear spin to interact with neighboring nuclei or ions, to lose its orientation) was calculated using the Laplace transform. Even though many researchers have investigated the problem of solving the NMR Bloch equations[17,18,19], deriving a general solution in terms of the relaxation time constants, is still a work in progress. For instance, analytical solutions were obtained for the square RF pulse and the hyperbolic-secant (HS) pulse with frequency-swept[25]. The use of the HS pulse was limited at the beginning of its application to the NMR for spin inversion only, however years later it was found out that it has a large utility on the Π-refocusing, as well as other flip angles ($\Pi/2$) for excitation. This is attributed to the two-dimensional (2D) spin-echo imaging work of Conolly et al[7]. It was also used in echo-planar imaging

* Corresponding author e-mail: hichem.el-euch@uphf.fr

(EPI), in which the HS pulse successfully recovers signal dropout caused by through-plane dephasing in the brain[28]. Another practical use of the HS pulse for spin excitation was proposed in the ultrashort echo-time MRI technique called SWIFT (Sweep Imaging with Fourier Transform) [15]. Later on, Zhang et al[29] derived full magnetizations "M_x, M_y, M_z" under HS pulse for spin resonance with an arbitrary initial condition.

Recently, Davydov et al [8] highlighted the necessity of deriving exact analytical solutions of the Bloch equations for nuclear magnetic resonance signals, for the case of liquids. Indeed, it was demonstrated [20,21,10,9,12,11] that, the relaxation times T_1 and T_2 in the recorded NMR signals offer a limited knowledge about the liquid medium as it shows only the presence of deviations from the standard state in it. Any other information is lost due to the lack of an appropriate model that provides a complete description of the recorded NMR signal. These drawbacks can only be overcome if an accurate analytical solution to the Bloch equations is available.

In addition to the Bloch equations[13,14,6], there is considerable interest in quantum computing based on the NMR. Early attempts to implement quantum computation with liquid crystals using weak and strong spin couplings were proposed[16]. Nuclear spins are used as qubits where, we can manipulate their quantum states to perform quantum operations such as single- and two-qubit gates with radio-frequency pulses and magnetic field gradients, respectively. Recently, other quantum computing possibilities have outperformed NMR-based approaches in terms of scalability and coherence times. Nevertheless, work on NMR-based quantum computing is still ongoing. It remains a valuable tool for exploring fundamental quantum phenomena, testing new quantum algorithms, and expanding our knowledge of quantum information processing. For instance, J. Reiner et al [23] successfully controlled electron and nuclear spins in a four-qubit register with phosphorus donors in silicon, demonstrating high fidelity. They achieved coherent control of electron spin qubits with T_2 = 12 μs and gate fidelities FG around 99.8% through optimized benchmarking. The control of both electron and nuclear spins in a multi-qubit register might enable the future development of small-scale algorithms. In another pertinent work based on solid-state NMR, C. E. Bradley et al [4] presented a new method for decoherence-protected gates that dynamically decouple electron spins and selectively drive nuclear spins. They created a ten-qubit quantum register with the electron spin of a nitrogen-vacancy center and nine nuclear spins in a diamond. Hence, they generated entanglement for up to seven qubits. In this context, exact solutions to the Bloch equations are critical for optimizing quantum computing. Indeed, by enabling precise simulation and modeling of complex quantum systems, these solutions provide an understanding of the system dynamics, and the noise effect, along with information loss and error generation. Nonetheless, pertinent analytical solutions for spectral line shapes involving multiple processes between two states and for steady-state behavior in certain systems were derived in [5]. These solutions have diverse applications, such as fitting line shapes, determining coalescence points, and developing simplified representations in scenarios of rapid exchange. Besides the limitation of the available methods capable of deriving exact solutions to the Bloch equations, our technique enables us to establish analytical solutions for the NMR signals for a variable RF magnetic field and a variable frequency. We believe that the strength and frequency of the RF field are important factors in controlling the behavior of nuclear spins in NMR signals. Indeed, the RF field is used to control the nuclear spin orientation. By applying specific RF pulses at precise frequencies, we can selectively excite the nuclear spin states to obtain desirable NMR signals. This might allow for precise control of the nuclear spin dynamics, resonance conditions, and pulse sequence design, and thereby achieve accurate NMR signals.

In this work, we derive the exact analytical solutions for the Bloch equations describing the configuration of the NMR signal line recorded in a weak (magnetic) field. Our study provides exact analytical solutions that consider variable " time-dependent" external radio-frequency magnetic field strength. Variable magnetization of the medium (experimentally it is the magnetic field of a spectrometer) and variable frequency shift caused by spatial variations in the magnetic field. Finally, we provided the numerical analysis of the NMR equations by taking various shaped magnetic fields in addition to the exact case derived by our method. For instance, we report the absorption dispersion signals for Sinusoidale and Eburp for a variable frequency shift.

The paper is structured as follows: in Section 2 we describe the Bloch equations of a recorded NMR signal in a weak magnetic field. In Section 3 we derive the solutions and analyze the results. Finally, concluding remarks are given in Section 4.

2 The Bloch equations of a recorded NMR signal in a weak magnetic field

The dynamics of the components of nuclear magnetizations in the presence of a spectrometer coil for NMR registration is given by [8,22,24,1]:

$$\frac{du(t)}{dt} + \frac{u(t)}{T_2} + v(t)\Delta\omega(t) = 0 \tag{1}$$

$$\frac{dv(t)}{dt} + \frac{v(t)}{T_2} - u(t)\Delta\omega(t) = -|\gamma|H_1(t)M_z \tag{2}$$

$$\frac{dM_z(t)}{dt} + \frac{M_z(t)}{T_1} - |\gamma|v(t)H_1 = \frac{M(t)}{T_1} \tag{3}$$

where T_1 is the spin-lattice relaxation time, and T_2 is the spin-spin relaxation time. H_1 is the detection field (radio-frequency field RF), and $\Delta\omega$ is the detuning frequency of the NMR signal from the magnetization precession frequency. γ is the gyromagnetic ratio of the nucleus.

Here u, v are the absorption and dispersion signals (see Table 1). M is the magnetization of the medium under study in the presence of the magnetic field (experimentally, it is the magnetic field of a spectrometer). $\Delta\omega$ represents the frequency shift caused by spatial variations in the magnetic field.

Realistic dynamical NMR variables and their physical relevance are summarized in Table 1. It is worth noting that our paper investigates the exact analytical solutions for all cases where $T_1 \neq T_2$ and out of the resonance. Nonetheless, the resonance case for $T_1 = T_2$ is solvable with our method. Besides, to get deeper insights on the scale, typical realistic values for the case of protons in water are: $\gamma = 2.675 \times 10^8\,\mathrm{rad\,s^{-1}\,T^{-1}}$ for the gyromagnetic ratio for protons, where T is the tesla unit. Furthermore, the typical magnetic field strength of 3 Tesla gives a Larmor frequency for protons in water as:

$$\omega_0 = 8.025 \times 10^8\,\mathrm{rad\,s^{-1}}$$

The strength of the magnetic field (B) in the Larmor frequency formula ($\omega_0 = \gamma B$) refers to the intensity of the main static magnetic field used in NMR (Nuclear Magnetic Resonance) experiments, and similarly in MRI (Magnetic Resonance Imaging) procedures. This magnetic field is typically established by the magnet within the imaging system. We will consider the values of our simulations at 3 Tesla.

3 Solutions and Analysis

Table 1: NMR dynamical variables

H_1	$\frac{\Gamma}{\gamma}$	RF external magnetic field of detection
M	$M_1 e^{-\alpha t}$	Magnetic field (spectrometer)
$\Delta\omega(t)$	$\beta \propto \chi$	Chirped frequency phase shift
$u(t)$	$u_1 e^{-\alpha t}$	Absorption signal
$v(t)$	$v_1 e^{-\alpha t}$	Dispersion signal
$M_z(t)$	$M_{z1}(t)e^{-\alpha t}$	Longitudinal magnetization

Our analysis is directed to the Bloch equations under a variable magnetic excitation and a chirped frequency shift ($\Delta\omega$ is time-dependent), u, v, and M_z are real. Then, we let $\alpha = \frac{1}{T_2}, \beta = \Delta\omega, \Gamma = |\gamma| H_1$ and $\lambda = \frac{1}{T_1}$. λ, α and γ are constants. β, Γ and M_1 are function of t. To solve the system of differential equations describing the Bloch equations, we introduce three new variables: v_1, u_1 and M_{z1} related to the previous $u(t)$, $v(t)$ and $M_z(t)$ as:

$$v_1(t) = v(t)e^{\alpha t} \tag{4}$$

$$u_1(t) = u(t)e^{\alpha t} \tag{5}$$

$$M_{z1}(t) = M_z(t)e^{\alpha t} \tag{6}$$

$$M_1(t) = M(t)e^{\alpha t} \tag{7}$$

By considering the new change of variable $x = \int \beta(t)dt$ and defining $g(x) = \frac{\Gamma}{\beta}$ Eq. (1), (2) and (3) become:

$$\frac{du_1}{dx} = -v_1(x) \tag{8}$$

$$\frac{dv_1}{dx} = u_1(x) - g(x)M_{z1}(x) \tag{9}$$

$$\frac{dM_{z1}}{dx} = g(x)v_1(x) + \frac{\alpha-\lambda}{\beta}M_{z1} + \frac{\lambda}{\beta}M_1 \tag{10}$$

This system of differential equations will serve as a basis for our future analysis to establish the exact solutions for the case where:

$$\beta = \frac{2c(\alpha-\lambda)e^{2(\alpha-\lambda)t}}{\left(1+ce^{2(\alpha-\lambda)t}\right)^2} \tag{11}$$

$$x = \frac{ce^{2(\alpha-\lambda)t}}{1+ce^{2(\alpha-\lambda)t}}, \tag{12}$$

$$\Gamma = \frac{2\sqrt{c}(\alpha-\lambda)e^{(\alpha-\lambda)t}}{(1+ce^{2(\alpha-\lambda)t})^2} \tag{13}$$

and

$$M_1 = \frac{2c^{\frac{5}{2}}(\alpha-\lambda)e^{5(\alpha-\lambda)t}}{\lambda(1+ce^{2(\alpha-\lambda)t})^3} \tag{14}$$

with c a positive constant. By repeated differentiation and substitution of the last three equations (8),(9) and (10) we get a linear third-order ordinary differential equation

$$\frac{d^3u_1}{dx^3} + \frac{1}{x}\frac{du_1}{dx} = x \tag{15}$$

Solving the last equation leads to expressions of $u_1(t), v_1(t)$ and $M_{z1}(t)$ in terms of Bessel functions (type 1 and 2).

$$u_1(x) = \frac{1}{3}x^3 + c_2xJ_2(2\sqrt{x}) + c_1xY_2(2\sqrt{x}) - x^2 + c_3 \tag{16}$$

$$v_1(x) = -\sqrt{x}\left[c_1Y_1(2\sqrt{x}) + c_2J_1(2\sqrt{x}) + x^{\frac{3}{2}} - 2\sqrt{x}\right] \tag{17}$$

$$M_{z1}(x) = \sqrt{\frac{x}{1-x}}\left[c_2xJ_2(2\sqrt{x}) + c_1xY_2(2\sqrt{x}) + \frac{1}{3}x^3 \right. \tag{18}$$
$$\left. c_2J_0(2\sqrt{x}) + c_1Y_0(2\sqrt{x}) - x^2 + 2x - 2 + c_3\right]$$

where supplementary c_1, c_2 and c_3 are constants, given in the annex, derived by considering the following initial conditions: $u_1(0) = 0, v_1(0) = 0$ and $M_{z1}(0) = 1$. In terms of the constant c, the solutions u(t), v(t) and $M_z(t)$

describing the behavior of nuclear magnetization in the magnetic field are:

$$
\begin{aligned}
v(t) = &-\frac{\sqrt{c}e^{(\alpha-\lambda)t}}{\sqrt{1+ce^{2(\alpha-\lambda)t}}}\Bigg[c_1 Y_1\Bigg(\frac{\sqrt{c}e^{(\alpha-\lambda)t}}{\sqrt{1+ce^{2(\alpha-\lambda)t}}}\Bigg)+ \\
&c_2 J_2\Bigg(\frac{\sqrt{c}e^{(\alpha-\lambda)t}}{\sqrt{1+ce^{2(\alpha-\lambda)t}}}\Bigg)+\frac{c^{\frac{3}{2}}e^{3(\alpha-\lambda)t}}{(1+ce^{2(\alpha-\lambda)t})^{\frac{3}{2}}}- \\
&\frac{\sqrt{c}e^{(\alpha-\lambda)t}}{\sqrt{1+ce^{2(\alpha-\lambda)t}}}\Bigg]e^{-\alpha t}
\end{aligned}
\tag{19}
$$

$v(t)$ represents the evolution of transverse magnetization and its interaction with the longitudinal magnetization M_z due to the T_2 relaxation and the external magnetic field H_1. This equation includes the effect of the radio frequency (RF) pulse ($\gamma H_1\ M_z$) in flipping the magnetization from the longitudinal to the transverse plane. v here is related to the terms λ and α that are, in their turns related to T_1 and T_2. This full analytical solution allows for obtaining the dispersion signal while considering various samples under the RF variable field, the variable frequency shift, and the variable magnetization.

$$
\begin{aligned}
u(t) = &\Bigg[\frac{c^3 e^{6(\alpha-\lambda)t}}{3(1+ce^{2(\alpha-\lambda)t})^3}+c_2\frac{ce^{2(\alpha-\lambda)t}J_2\Big(\frac{\sqrt{c}e^{(\alpha-\lambda)t}}{\sqrt{1+ce^{2(\alpha-\lambda)t}}}\Big)}{1+ce^{2(\alpha-\lambda)t}}+ \\
&c_1\frac{ce^{2(\alpha-\lambda)t}Y_2\Big(\frac{\sqrt{c}e^{(\alpha-\lambda)t}}{\sqrt{1+ce^{2(\alpha-\lambda)t}}}\Big)}{1+ce^{2(\alpha-\lambda)t}}-\frac{c^2 e^{4(\alpha-\lambda)t}}{(1+ce^{2(\alpha-\lambda)t})^2}+ \\
&c_3\Bigg]e^{-\alpha t}
\end{aligned}
\tag{20}
$$

We recall that $u(t)$ describes the nuclear magnetization precession in the presence of the magnetic field with the transverse relaxation time T_2. This decay is primarily due to the interactions between the spins of adjacent nuclei, which result in energy exchange and, eventually, relaxation. Our solution is in terms of λ and α. These terms are the inverse decay rates.

$$
\begin{aligned}
M_z(t) = &\frac{1}{24Y_1(\sqrt{2})J_0(\sqrt{2})-24J_1(\sqrt{2})Y_0(\sqrt{2})} \\
&\Bigg[8\frac{\sqrt{c}e^{(\alpha-\lambda)t}}{\sqrt{1+ce^{2(\alpha-\lambda)t}}}\frac{1}{\sqrt{1-\frac{ce^{2(\alpha-\lambda)t}}{\sqrt{1+ce^{2(\alpha-\lambda)t}}}}}\Bigg(\\
&\frac{1}{4}\Bigg(\Big(\frac{9ce^{2(\alpha-\lambda)t}}{1+ce^{2(\alpha-\lambda)t}}-9\Big)(\sqrt{2}Y_0(\sqrt{2})-\frac{8}{3}Y_1(\sqrt{2})) \\
&J_0\Bigg(\frac{2\sqrt{c}e^{(\alpha-\lambda)t}}{\sqrt{1+ce^{2(\alpha-\lambda)t}}}\Bigg)\Bigg)-\frac{1}{4}(9\sqrt{2}J_0(\sqrt{2})-24J_1(\sqrt{2})) \\
&\Bigg(\frac{ce^{2(\alpha-\lambda)t}}{1+ce^{2(\alpha-\lambda)t}}-1\Bigg)Y_0\Bigg(\frac{2\sqrt{c}e^{(\alpha-\lambda)t}}{\sqrt{1+ce^{2(\alpha-\lambda)t}}}\Bigg)\Bigg)- \\
&\frac{9}{4}\frac{\sqrt{c}e^{(\alpha-\lambda)t}}{\sqrt{1+ce^{2(\alpha-\lambda)t}}}(\sqrt{2}Y_0(\sqrt{2})-\frac{8}{3}Y_1(\sqrt{2})) \\
&J_1\Bigg(\frac{2\sqrt{c}e^{(\alpha-\lambda)t}}{\sqrt{1+ce^{2(\alpha-\lambda)t}}}\Bigg)+\frac{9}{4}\frac{\sqrt{c}e^{(\alpha-\lambda)t}}{\sqrt{1+ce^{2(\alpha-\lambda)t}}} \\
&(\sqrt{2}J_0(\sqrt{2})-\frac{8}{3}J_1(\sqrt{2}))Y_1\Bigg(\frac{2\sqrt{c}e^{(\alpha-\lambda)t}}{\sqrt{1+ce^{2(\alpha-\lambda)t}}}\Bigg)+ \\
&(Y_1(\sqrt{2})J_0(\sqrt{2})-J_1(\sqrt{2})Y_0(\sqrt{2})) \\
&\Bigg(\frac{c^3e^{6(\alpha-\lambda)t}}{(1+ce^{2(\alpha-\lambda)t})^3}-\frac{3c^2e^{4(\alpha-\lambda)t}}{(1+ce^{2(\alpha-\lambda)t})^2}+ \\
&\frac{6ce^{2(\alpha-\lambda)t}}{1+ce^{2(\alpha-\lambda)t}}-\frac{37}{8}\Bigg)\Bigg)e^{-\alpha t}\Bigg]
\end{aligned}
\tag{21}
$$

Finally, $M_z(t)$ gives the evolution of the longitudinal magnetization (M_z), considering its relaxation toward equilibrium with a time constant T_1.
Besides, we can notice from Eq. (13) that the constant c is related to the initial magnetic field strength, and depends on T_1 and T_2. In fact, at t=0s, we can write:

$$
M_0 = (\frac{\alpha-\lambda}{\lambda})(\frac{2c^{5/2}}{(1+c)^3}) \tag{22}
$$

In our work, the initial magnetization M_0 value was

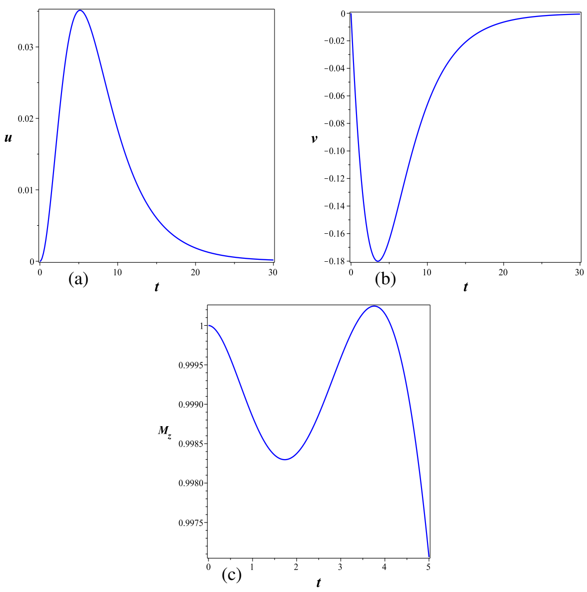

Fig. 1: (a) Exact analytical solutions for the line shapes: the absorption signal. (b) The dispersion signal. (c) The transverse magnetization signal with parameters $T_1 = 29.4\,s$, $T_2 = 4.2\,s$, Carbon-13 (^{13}C) in liquid-state quaternary carbons, where weak dipole interactions and chemical shift anisotropy are the dominant relaxation mechanism. $M_0 = 1\,T$.

taken equal to 1. Nevertheless, we can solve the equations for another initial condition of M_0 different from 1. Indeed, we replace in Eq.(22) by T_1 and the T_2 values, then we deduce the free mathematical parameter c. After getting c,

we write u, v and M.
Hence, the solutions can be obtained for various values of T_1 and the T_2.

Figure 1 shows the exact analytical solutions of the Bloch equations for the NMR signals under the time-dependent RF field, chirped frequency shift, and variable magnetization. (a) presents the absorption signal $u(t)$, which increases from zero, reaches a maximum around $t = 5$ s, and then gradually decays. (b) displays the dispersion signal $v(t)$, which exhibits a symmetric lineshape with respect to the absorption signal. (c) shows the time evolution of the longitudinal magnetization $M_z(t)$, which starts at its initial value and relaxes toward equilibrium while being affected by the RF excitation.

Figure 2 compares the temporal dynamics of the exact solutions $u(t)$, $v(t)$, and $M_z(t)$ for two different samples with $M_0 = 1$ T. Panels (a)–(c) correspond to the light hydrocarbon liquid (e.g., light alkanes or kerosene) case ($T_1 \approx 3.2$ s, $T_2 \approx 0.8$ s), while panels (d)–(f) correspond to partially deoxygenated blood ($T_1 \approx 1.35$ s, $T_2 \approx 0.05$ s).

In (a) and (d), the absorption signals $u(t)$ are shown. The signal of deoxygenated blood reaches its maximum absorption faster than oil due to its shorter T_1. Panels (b) and (e) display the dispersion signals $v(t)$, which also evolve more rapidly in the blood sample. Finally, panels (c) and (f) show the longitudinal magnetization $M_z(t)$. The shorter T_1 leads to a faster recovery of M_z toward equilibrium compared to the oil sample.

Next, In Fig 3, we consider different RF pulses. The exact analytical solution in Eq.(13) depends on T_1 and T_2. This pulse is the EXpulse (exact solution pulse) and is plotted by the blue curve for $T_1 = 2.05s$ and $T_2 = 0.5s$ could represent the case of water in Coarse Sandstone. The red plot designates the Eburp pulse commonly used in NMR systems[26]. The dashed curve is for the Sine pulse. In Figs.4 (a), (b), and (c), we report the absorption, dispersion, and magnetization signals for different excitation pulses. We observe that peaks and time differ across various scenarios. Interestingly, the magnetization signal is almost identical for Eburp and EX pulses whereas, the absorption and dispersion are the same for a short excitation time. Hence, our Exact solution for the ”EX pulse” can represent the Eburp pulse for short excitation time. Finally, we expect that our solutions offer a framework for obtaining NMR signals under variable frequency, variable excitation, and variable magnetization.

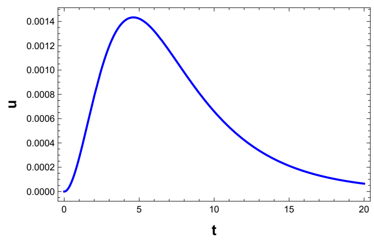

(a)

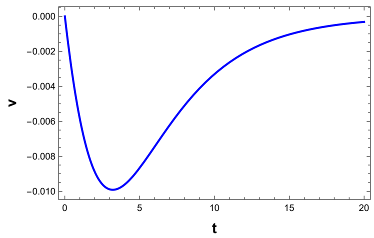

(b)

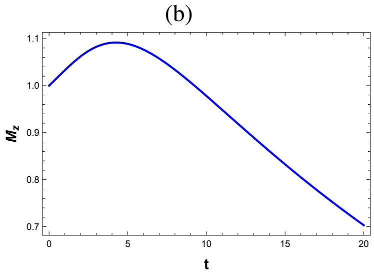

(c)

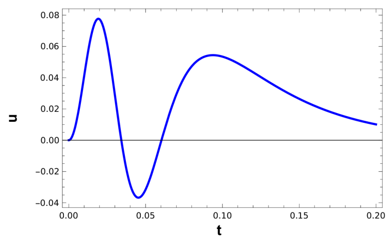

(d)

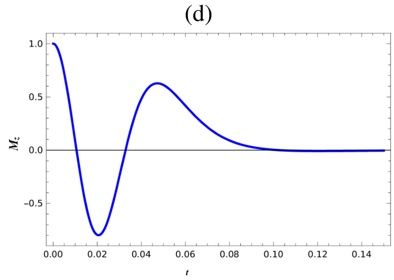

(e)

4 Conclusion

In this paper, we establish exact analytical solutions to the Bloch equations describing the nuclear magnetic resonance NMR signal in which the external radio-frequency magnetic field is time-variable, the medium’s magnetization is also time-dependent, and the

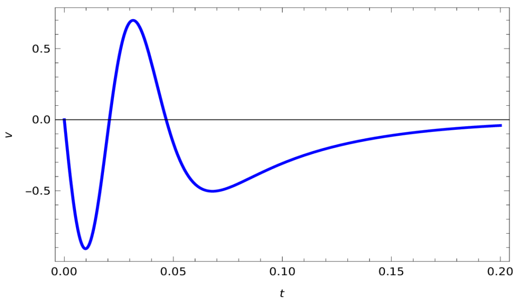

(f)

Fig. 2: Temporal dynamics of the exact solutions u, v, M for $M_0 = 1$ Tesla. Panels (a)–(c): the light hydrocarbon liquid (e.g., light alkanes or kerosene) case with $T_1 \approx 3.2s$, $T_2 \approx 0.8s$. Panels (d)–(f): partially deoxygenated blood case with $T_1 \approx 1.35s$, $T_2 \approx 0.05s$.

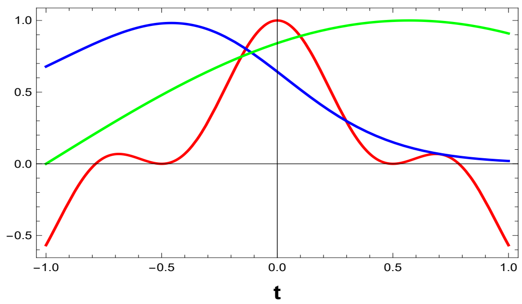

Fig. 3: Shape of NMR pulses with T_2=0.5s, T_1=2.05s, Eburp pulse (Red Curve —), Sin pulse (Green Curve —) and our exact solution: EXpulse (Blue Curve —).

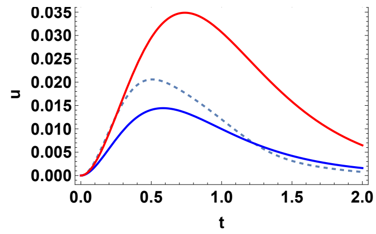

(a) Absorption signal

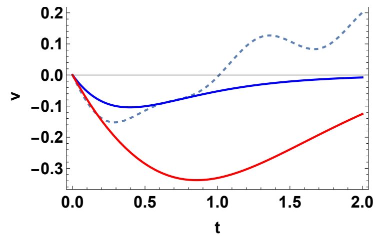

(b) Dispersion signal

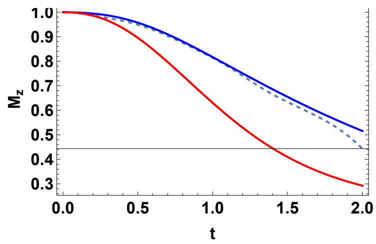

(c) Magnetization

Fig. 4: (a) The absorption signal, (b) the dispersion signal and (c) the magnetization

frequency shift is chirped. Hence, we obtained the expressions of the absorption and dispersion signals. Additionally, we obtained the evolution of the longitudinal magnetization (M_z) in terms of the relaxation time T_1 and T_2. We derived these signals numerically for two RF excitations, Eburp and Sine, which we compare to our exact pulse solution (represented by the EX pulse). We observe that for a short excitation time, the EX pulse is almost identical to the Eburp pulse for absorption and dispersion, while the obtained magnetization is the same for both of them. Beyond providing exact solutions, the present work offers a general mathematical framework for investigating NMR dynamics under simultaneously varying excitation amplitudes, magnetic field, and frequency modulation. The explicit dependence of the solutions on the relaxation parameters also makes them potentially useful for future analytical and numerical studies. More broadly, the analytical methodology introduced here is not restricted to conventional NMR spectroscopy. It may also find applications in nonlinear dynamics. Future work will focus on extending the present approach to more general experimental conditions and more general classes of shaped radio-frequency pulses.

References

[1] Abragam, A. The Principles of Nuclear Magnetism. (1961).
[2] Awojoyogbe, OB. Analytical solution of the time-dependent Bloch NMR flow equations: a translational mechanical analysis. Physica A: Statistical Mechanics and Its Applications. 339,3-4, 437-460 (2004).
[3] Bloch, Felix. Nuclear induction. Physical review. 70,7-8, 460 (1946).
[4] Bradley, Conor E and Randall, Joe and Abobeih, Mohamed H and Berrevoets, RC and Degen, MJ and Bakker, Michiel A and Markham, Matthew and Twitchen, DJ and Taminiau, Tim H. A ten-qubit solid-state spin register with quantum memory up to one minute. Physical Review X 9,3, 031045 (2019).
[5] Březina, Václav and Hanyková, Lenka and Velychkivska, Nadiia and Hill, Jonathan P and Labuta, Jan. NMR lineshape analysis using analytical solutions of multi-state chemical

exchange with applications to kinetics of host–guest systems. Scientific Reports 12,1, 17369 (2022).
[6] Boutabba, N and Grira, S and Eleuch, H. Analysis of a q-deformed hyperbolic short laser pulse in a multi-level atomic system. Scientific Reports. 12,1, 9308 (2022).
[7] Conolly, Steven and Nishimura, Dwight and Macovski, Albert. A selective adiabatic spin-echo pulse. Journal of Magnetic Resonance. 83,2, 324-334 (1989).
[8] Davydov, MN and Davydov, VV and Rud, V Yu. On necessity for analytical solution of the Bloch equations for nuclear magnetic resonance signals at condition express control of liquid medium. Journal of Physics: Conference Series 2086,1, 012134 (2021).
[9] Davydov, VV. Control of the longitudinal relaxation time T 1 of a flowing liquid in NMR flowmeters. Russian Physics Journal. 42, 9, 822-825 (1999).
[10] Davydov, VV and Velichko, EN and Dudkin, VI and Karseev, A Yu. A nutation nuclear-magnetic teslameter for measuring weak magnetic fields. Measurement Techniques 54,684-689 (2014).
[11] Davydov, VV and Velichko, EN and Dudkin, VI and Karseev, A Yu. A nuclear magnetic relaxometer for express testing of the condensed medium conditions. Instruments and Experimental Techniques. 58, 234-238 (2015).
[12] Gizatullin, Bulat and Gafurov, Marat and Vakhin, Alexey and Rodionov, Alexander and Mamin, Georgy and Orlinskii, Sergei and Mattea, Carlos and Stapf, Siegfried. Native vanadyl complexes in crude oil as polarizing agents for in situ proton dynamic nuclear polarization. Energy & Fuels. 33, 11, 10923-10932 (2019).
[13] Grira, Sofiane and Boutabba, Nadia and Eleuch, Hichem. Exact solutions of the Bloch equations of a two-level atom driven by the generalized double exponential quotient pulses with dephasing. Mathematics. 10,12, 2105 (2022).
[14] Grira, Sofiane and Boutabba, Nadia and Eleuch, Hichem. Exact Solutions of the Bloch Equations to the Asymmetric Hyperbolic Cosine Pulse with Chirped Frequency. Mathematics. 11,9, 2159 (2023).
[15] Idiyatullin, Djaudat and Corum, Curt and Park, Jang-Yeon and Garwood, Michael. Fast and quiet MRI using a swept radiofrequency. Journal of magnetic resonance. 181,2, 342-349 (2006).
[16] Jones, Jonathan A. Quantum computing with NMR. Progress in nuclear magnetic resonance spectroscopy. 59,2, 91-120 (2011).
[17] Madhu, PK and Kumar, Anil. Direct Cartesian-space solutions of generalized Bloch equations in the rotating frame. Journal of Magnetic Resonance, Series A 114,2, 201-211 (1995).
[18] Madhu, PK and Kumar, Anil. Bloch equations revisited: New analytical solutions for the generalized Bloch equations. Concepts in Magnetic Resonance: An Educational Journal 9,1,1-12 (1997).
[19] Morris, GARETH A and Chilvers, PAUL B. General analytical solutions of the Bloch equations. Journal of Magnetic Resonance, Series A 107,2,236-238 (1994).
[20] Myazin, NS and Davydov, VV and Rud, V Yu and Yushkova, VV and Dudkin, VI. New method for determining the composition of liquid media during the express control of their state using the nuclear magnetic resonance phenomena. Journal of Physics: Conference Series. 1400, 6,066008 (2019).
[21] Myazin, NS and Davydov, VV and Yushkova, VV and Glinushkin, AP and Taranda, NI and Rud, V Yu. On the need to control the state of the flowing media by the values of relaxation constants. Journal of Physics: Conference Series. 1410,1, 012130 (2019).
[22] Packard, ME and Varian, RH. Free nuclear induction in the Earth's magnetic field. Phys Rev. 93 (1954).
[23] Reiner, J and Chung, Y and Misha, SH and Lehner, C and Moehle, C and Poulos, D and Monir, S and Charde, KJ and Macha, P and Kranz, L and others. High-fidelity initialization and control of electron and nuclear spins in a four-qubit register. Nature Nanotechnology. 1-7 (2024).
[24] Rukin, EV and Myazin, NS and Davydov, VV and Dudkin, VI and Rud, V Yu. Modeling of non-stationary processes in the study of liquid media by the method of nuclear magnetic resonance in a weak field. Journal of Physics: Conference Series. 1368,4, 042011 (2019).
[25] Silver, MS and Joseph, RI and Hoult, DI. Selective spin inversion in nuclear magnetic resonance and coherent optics through an exact solution of the Bloch-Riccati equation. Physical review A. 31,4, 2753 (1985).
[26] Stott, Katherine and Stonehouse, Jonathan and Keeler, James and Hwang, Tsang-Lang and Shaka, AJ. Excitation sculpting in high-resolution nuclear magnetic resonance spectroscopy: application to selective NOE experiments. Journal of the American Chemical Society. 117, 14, 4199-4200 (1995).
[27] Torrey, HC. Transient nutations in nuclear magnetic resonance. Physical Review. 76,8, 1059 (1949).
[28] Wastling, Stephen J and Barker, Gareth J. Designing hyperbolic secant excitation pulses to reduce signal dropout in gradient-echo echo-planar imaging. Magnetic resonance in medicine. 74,3, 661-672 (2015).
[29] Zhang, Jinjin and Garwood, Michael and Park, Jang-Yeon. Full analytical solution of the bloch equation when using a hyperbolic-secant driving function. Magnetic resonance in medicine. 77,4, 6030-6038 (2017).

Annex: Supplementary Equations

The following expressions define the integration constants C_1, C_2, and C_3 derived from the initial conditions $u_1(0) = 0$, $v_1(0) = 0$, and $M_{z1}(0) = 1$.

$$C_1 = \frac{K_1}{K_2} \tag{23}$$

where K_1 and K_2 are given by

$$\begin{aligned} K_1 = -\Bigg[& J_1\left(2\sqrt{\frac{c}{1+c}}\right) c\sqrt{1+c} + 2J_1\left(2\sqrt{\frac{c}{1+c}}\right) c\sqrt{\frac{c}{1+c}} - J_0\left(2\sqrt{\frac{c}{1+c}}\right) c^2 + \\ & J_1\left(2\sqrt{\frac{c}{1+c}}\right) \sqrt{1+c} + 2J_1\left(2\sqrt{\frac{c}{1+c}}\right) \sqrt{\frac{c}{1+c}} - 2cJ_0\left(2\sqrt{\frac{c}{1+c}}\right) \Bigg] \end{aligned}$$

$$\begin{aligned} K_2 = & \sqrt{\frac{c}{1+c}} J_0\left(2\sqrt{\frac{c}{1+c}}\right) c^2 Y_1\left(2\sqrt{\frac{c}{1+c}}\right) - J_1\left(2\sqrt{\frac{c}{1+c}}\right) Y_0\left(2\sqrt{\frac{c}{1+c}}\right) c^2 + \\ & 2J_0\left(2\sqrt{\frac{c}{1+c}}\right) cY_1\left(2\sqrt{\frac{c}{1+c}}\right) - 2J_1\left(2\sqrt{\frac{c}{1+c}}\right) Y_0\left(2\sqrt{\frac{c}{1+c}}\right) c + \\ & J_0\left(2\sqrt{\frac{c}{1+c}}\right) Y_1\left(2\sqrt{\frac{c}{1+c}}\right) - J_1\left(2\sqrt{\frac{c}{1+c}}\right) Y_0\left(2\sqrt{\frac{c}{1+c}}\right) \end{aligned}$$

$$C_2 = \frac{K_3}{K_2} \tag{24}$$

where K_3 is given by

$$\begin{aligned} K_3 = & Y_1\left(2\sqrt{\frac{c}{1+c}}\right) c\sqrt{1+c} + 2Y_1\left(2\sqrt{\frac{c}{1+c}}\right) c\sqrt{\frac{c}{1+c}} - Y_0\left(2\sqrt{\frac{c}{1+c}}\right) c^2 + \\ & Y_1\left(2\sqrt{\frac{c}{1+c}}\right) \sqrt{1+c} + 2Y_1\left(2\sqrt{\frac{c}{1+c}}\right) \sqrt{\frac{c}{1+c}} - 2cY_0\left(2\sqrt{\frac{c}{1+c}}\right) \end{aligned}$$

$$C_3 = \frac{K_4}{K_5} \tag{25}$$

where K_4 and K_5 are given by

$$\begin{aligned} K_4 = -c\Bigg[& -2Y_1\left(2\sqrt{\frac{c}{1+c}}\right) J_0\left(2\sqrt{\frac{c}{1+c}}\right) c^2\sqrt{\frac{c}{1+c}} + 2J_1\left(2\sqrt{\frac{c}{1+c}}\right) Y_0\left(2\sqrt{\frac{c}{1+c}}\right) c^2\sqrt{\frac{c}{1+c}} + \\ & 3Y_1\left(2\sqrt{\frac{c}{1+c}}\right) J_2\left(2\sqrt{\frac{c}{1+c}}\right) c\sqrt{1+c} + 6Y_1\left(2\sqrt{\frac{c}{1+c}}\right) J_2\left(2\sqrt{\frac{c}{1+c}}\right) c\sqrt{\frac{c}{1+c}} - \\ & 3Y_1\left(2\sqrt{\frac{c}{1+c}}\right) J_0\left(2\sqrt{\frac{c}{1+c}}\right) c\sqrt{\frac{c}{1+c}} - 3J_1\left(2\sqrt{\frac{c}{1+c}}\right) Y_2\left(2\sqrt{\frac{c}{1+c}}\right) c\sqrt{1+c} - \\ & 6J_1\left(2\sqrt{\frac{c}{1+c}}\right) Y_2\left(2\sqrt{\frac{c}{1+c}}\right) c\sqrt{\frac{c}{1+c}} + 3J_1\left(2\sqrt{\frac{c}{1+c}}\right) Y_0\left(2\sqrt{\frac{c}{1+c}}\right) c\sqrt{\frac{c}{1+c}} + \\ & 3Y_2\left(2\sqrt{\frac{c}{1+c}}\right) J_0\left(2\sqrt{\frac{c}{1+c}}\right) c^2 - 3Y_0\left(2\sqrt{\frac{c}{1+c}}\right) J_2\left(2\sqrt{\frac{c}{1+c}}\right) c^2 + \\ & 3Y_1\left(2\sqrt{\frac{c}{1+c}}\right) J_2\left(2\sqrt{\frac{c}{1+c}}\right) \sqrt{1+c} + 6Y_1\left(2\sqrt{\frac{c}{1+c}}\right) J_2\left(2\sqrt{\frac{c}{1+c}}\right) \sqrt{\frac{c}{1+c}} - \\ & 3J_1\left(2\sqrt{\frac{c}{1+c}}\right) Y_2\left(2\sqrt{\frac{c}{1+c}}\right) \sqrt{1+c} - 6J_1\left(2\sqrt{\frac{c}{1+c}}\right) Y_2\left(2\sqrt{\frac{c}{1+c}}\right) \sqrt{\frac{c}{1+c}} + \\ & 6Y_2\left(2\sqrt{\frac{c}{1+c}}\right) J_0\left(2\sqrt{\frac{c}{1+c}}\right) c - 6J_2\left(2\sqrt{\frac{c}{1+c}}\right) Y_0\left(2\sqrt{\frac{c}{1+c}}\right) c \Bigg] \end{aligned}$$

$$K_5 = 3\left(c^3 + 3c^2 + 3c + 1\right)\left(Y_1\left(2\sqrt{\frac{c}{1+c}}\right) J_0\left(2\sqrt{\frac{c}{1+c}}\right) - Y_0\left(2\sqrt{\frac{c}{1+c}}\right) J_1\left(2\sqrt{\frac{c}{1+c}}\right) \sqrt{\frac{c}{1+c}}\right) \tag{26}$$

Nadia Boutabba is a physicist and academic specializing in quantum optics, optoelectronics, and photonics. She currently serves as Maître de Conférences (Associate Professor) at the Université Polytechnique Hauts-de-France, affiliated with the LAMIH laboratory: LAMIH UMR CNRS 8201. Her research focuses on non-linear optics, laser-matter interactions, quantum optics, and photonics. Dr. Boutabba earned her Ph.D. in Quantum Physics in 2006 from the University of Tunis El Manar, Tunisia, with a thesis on photovoltaic conversion under high-intensity light in polymer materials. She obtained her Master's degree in Quantum Optoelectronics (Quantum Well Laser Diodes) in 2000 from the University of Carthage, Tunisia. She previously served as a Visiting Assistant Professor at Texas And M University and worked for five years at Cégep Saint-Laurent in Montreal, Canada. Dr. Boutabba has authored and co-authored numerous scientific publications in the fields of quantum optics and photonics.

Sofiane Grira is an Associate Professor of Mathematics at Al Akhawayn University in Ifrane, Morocco. He holds a Ph.D. in Mathematics from the Université de Sherbrooke, Canada (2002). Prior to joining Al Akhawayn University, he served as Associate Professor of Mathematics at Abu Dhabi University, United Arab Emirates, for nearly two decades. With over twenty years of experience in higher education, Dr. Grira has taught a broad range of courses in Mathematics and Statistics to Engineering and Information Technology students, with a sustained commitment to integrating technology into pedagogy and curriculum development. His research interests span Applied Mathematics, Stochastic Processes, Probability Theory, Mathematical Physics — Bolch Equations — Game Theory, and Mathematics Education. He has secured multiple research grants and published in internationally indexed journals, with collaborative work extending across Mathematics, Physics, and Computer Science.

Hichem Eleuch is a Professor-Chair of Excellence in Quantum Information and Artificial Intelligence at the University Polytechnique Hauts-de-France in Valenciennes, France. He earned his Ph.D. in Quantum Physics from the Kastler Brossel Laboratory (École Normale Supérieure and Pierre and Marie Curie University – now Sorbonne University) in Paris, France, and holds a Diplom-Ingenieur (BS+MSc) in Electrical Engineering and Information Technology from the Technical University of Munich, Germany. His career includes positions and research visits at Texas A&M University, the Max Planck Institute, Princeton University, McGill University, and other leading institutions. Dr. Eleuch has authored over 300 peer-reviewed papers and holds 21 U.S. patents. He is a Fellow of the African Academy of Sciences, a Member of the Mohammed Bin Rashid Academy of Scientists, and a Member of The World Academy of Sciences (TWAS). His distinctions include the 2023 Prize of Excellence from the Arab Physical Society and the Abdul Hameed Shoman Prize in Quantum Physics.